ELSEVIER

Chemical Engineering Journal 138 (2008) 628–633

Chemical Engineering Journal

www.elsevier.com/locate/cej

Short communication

Mass transfer enhancement by chemical reaction in turbulent tube flow

Carlos A. Ramírez *

Department of Chemical Engineering, University of Puerto Rico, Mayagüez, Puerto Rico 00681-9046

Received 15 August 2007; received in revised form 2 October 2007; accepted 5 October 2007

Abstract

Section 21.4 of *Transport Phenomena* (BSL2 after its three authors: Bird, Stewart, and Lightfoot; second ed.; full reference given in [1]) addresses the problem of mass transfer enhancement by a homogeneous and irreversible first-order chemical reaction in turbulent tube flow. The authors discuss several solution approaches of historical interest, and provide a complete transport model for solute A based on the laws of conservation of mass and momentum, from which the local Sherwood number, *Sh*, can be obtained as a function of the dimensionless axial distance into the mass transfer zone and the Damköhler number, *Da*. The latter accounts for the effect of reaction kinetics on solute transport. However, BSL2 is very sketchy in the solution details of their model, and does not validate the key results relative to other studies. Thus, the usefulness of the authors' modelling approach cannot be properly assessed. In this work, a fully documented numerical solution of the original transport problem is given, along with comprehensive results such as velocity and concentration profiles, as well as *Sh* values outside the range of axial positions given in BSL2. Mass transfer enhancement factors (ratio of *Sh* with chemical reaction/*Sh* without reaction) are also calculated and compared with the literature. Our results show that accurate estimates of enhancement factors in turbulent tube flow with chemical reaction can be obtained using the straightforward BSL2 modelling approach, which may be readily adapted to examine other situations relevant to chemical engineering.

Keywords: Mass transfer; Fluid mechanics; Turbulent tube flow; Homogeneous and irreversible chemical reaction; Mathematical modelling; Local Sherwood number

1. Introduction

This communication provides full documentation and comprehensive results, extends the range of applicability of the solution, and places in perspective the turbulent mass transfer problem with chemical reaction presented in §21.4 of the classic *Transport Phenomena* text [1], hereinafter referred to as BSL2. In this section, Bird et al. discuss the academically challenging and industrially relevant topic of mass transfer enhancement by a chemical reaction in turbulent tube flow. One of the problems analyzed is that of a steadily driven turbulent flow in which the wall material (solid species A) is only slightly soluble in the tube fluid (liquid species B). Upon dissolution at the wall, mass transfer of A in the tube fluid by axial convection and radial diffusion ensues, accompanied by a homogeneous and irreversible first-order chemical reaction (A → products). Assumptions include isothermal operation, constant fluid physical properties, and a fully developed turbulent *velocity* profile. Simplified versions of this problem have been tackled by several authors (see pertinent references in [1], pp. 659 and 661), with all of them predicting mass transfer enhancement from the wall as a result of the chemical reaction in the tube fluid.

Avoiding the shortcomings of earlier studies, BSL2 presents Eq. (21.4-12) which is the steady, time-smoothed mass conservation equation for solute A in liquid B, given below in its original form:

$$v^+ \frac{\partial C}{\partial z^+} = \frac{1}{r^+} \frac{\partial}{\partial r^+} \left[r^+ \left(\frac{1}{Sc} + (l^+)^2 \left| \frac{\mathrm{d}v^+}{\mathrm{d}r^+} \right| \right) \frac{\partial C}{\partial r^+} \right] - Da\, C \tag{21.4-12}$$

In this equation, the dimensionless molar concentration of A, $C(r^+, z^+)$, appears as a function of the dimensionless radial (r^+) and axial (z^+) distances, with the Schmidt (*Sc*) and Damköhler (*Da*) numbers as either known or user-specified parameters. *Sc* relates the rate of momentum transfer to that of solute dif-

* Tel.: +787 832 4040x2561.
E-mail address: cramirez@uprm.edu.

1385-8947/$ – see front matter © 2007 Elsevier B.V. All rights reserved.
doi:10.1016/j.cej.2007.10.008

Nomenclature

Notation

C dimensionless molar concentration of solute A in the tube fluid $= \bar{c}_A/c_{A0}$

$\bar{c}_A$ time-smoothed molar concentration of solute A in the tube fluid

c_{A0} molar concentration of solute A on the fluid side of the tube wall interface

Da Damköhler number $= k_1'''\upsilon/v_*^2 = 0$, 0.001, or 0.01; dimensionless

D_{AB} binary diffusion coefficient of solute A in liquid B

f Fanning friction factor for turbulent tube flow given by the Blasius equation (BSL2 Eq. (6.2-12); valid for $2100 < Re < 100000$) $= 0.0791/Re^{1/4} = 0.00791$ for $Re = 10000$; dimensionless

k_1''' rate constant for a homogeneous and irreversible first-order chemical reaction (A → products)

k_c mass transfer coefficient defined by BSL2 Eq. (21.4-2)

l mixing length for turbulent tube flow given by BSL2 Eq. (5.4-7)

l^+ dimensionless mixing length for turbulent tube flow $= lv_*/\upsilon$

r radial distance measured from the tube centerline

r^+ dimensionless radial distance measured from the tube centerline $= rv_*/\upsilon$

R tube radius

R^+ dimensionless distance of the tube centerline measured from the wall $= Rv_*/\upsilon = R\langle\bar{v}_z\rangle(f/2)^{1/2}/\upsilon = (Re/2)(f/2)^{1/2} = 314.44$ for $Re = 10000$ and $f = 0.00791$

Re Reynolds number for fully developed turbulent tube flow $= 2R\langle\bar{v}_z\rangle/\upsilon = 10000$; dimensionless

Sc Schmidt number $= \upsilon/D_{AB} = 200$; dimensionless

Sh local Sherwood number given by the dimensionless form of BSL2 Eq. (21.4-2) $= \frac{2Rk_c}{D_{AB}} = \frac{-2R^+\partial C/\partial y^+(0,x)}{1-C(R^+,x)}$; dimensionless

$\bar{v}_z$ time-smoothed z-component (axial) of the velocity for fully developed turbulent tube flow

v^+ dimensionless time-smoothed z-component (axial) of the velocity for fully developed turbulent tube flow $= \bar{v}_z/v_*$

v_* friction velocity $= \langle\bar{v}_z\rangle(f/2)^{1/2}$ obtained from BSL2 Eq. (6.1-4a)

$\langle\bar{v}_z\rangle$ time-smoothed z-component (axial) of the velocity for fully developed turbulent tube flow averaged over the tube cross section

x transformed dimensionless axial distance into the mass transfer zone measured from the tube inlet $= \log_{10}(z^+ + 1)$; note that $x(0) = 0$ which is a convenient starting point for the numerical solution of the problem

y distance into the fluid measured from the tube wall $= R - r$

y^+ dimensionless distance into the fluid measured from the tube wall $= yv_*/\upsilon = R^+ - r^+$

z axial distance into the mass transfer zone measured from the tube inlet

z^+ dimensionless axial distance into the mass transfer zone measured from the tube inlet $= zv_*/\upsilon$

Greek letters

ϕ mass transfer enhancement factor = asymptotic value of Sh with chemical reaction to that without reaction; dimensionless

υ kinematic viscosity of the tube fluid (dilute solution of all chemical species in liquid B)

fusion, while Da includes the effect of reaction kinetics. To solve BSL2 Eq. (21.4-12) for $C(r^+, z^+)$, the velocity profile for fully developed turbulent tube flow is needed. This appears explicitly as v^+ in the convective term on the left side (which allows for the axial development of the concentration profile) and in the radial derivative $|dv^+/dr^+|$ on the right side. The equation also includes the van Driest model for the mixing length, l^+, as modified by Hanna et al. after fitting heat and mass transfer data from drag reduction experiments [2]. The dimensionless axial velocity profile v^+ may be obtained by integrating the time-smoothed equation of motion for steadily driven tube flow which also includes l^+ (BSL2 Eqs. (21.4-13) and (21.4-14)):

$$(l^+)^2\left(\frac{dv^+}{dy^+}\right)^2 + \frac{dv^+}{dy^+} = 1 - \frac{y^+}{R^+} \tag{21.4-13}$$

$$l^+ = 0.4y^+\frac{1 - \exp(-y^+/26)}{[1 - \exp(-0.26y^+)]^{1/2}} \tag{21.4-14}$$

In these equations, R^+ is the dimensionless distance of the tube centerline measured from the wall, and $y^+ = R^+ - r^+$ is the dimensionless distance into the fluid measured from the tube wall. Standard velocity boundary conditions include no-slip at the wall and symmetry at the tube centerline, while the dimensionless molar concentration of A is taken as $C = 0$ at the tube inlet, $C = 1$ on the fluid side of the wall interface, and symmetric at the tube centerline. The problem was solved by a former student of Prof. Warren E. Stewart several years ago (Michael Caracotsios, presently Adjunct Professor of Chemical Engineering, Illinois Institute of Technology, Chicago, IL), but the results were never published. The only record of the numerical solution of the three equations presented above is BSL2 Fig. 21.4-1 ([1], p. 662; reproduced here), in which the local Sherwood number, Sh, calculated from the dimensionless form of BSL2 Eq. (21.4-2), is given as a function of z^+ for a turbulent Reynolds number, Re, of 10000, $Sc = 200$, and $Da = 0$, 0.001, and 0.01. Their results show decreasing values of Sh into the mass transfer zone, with considerable

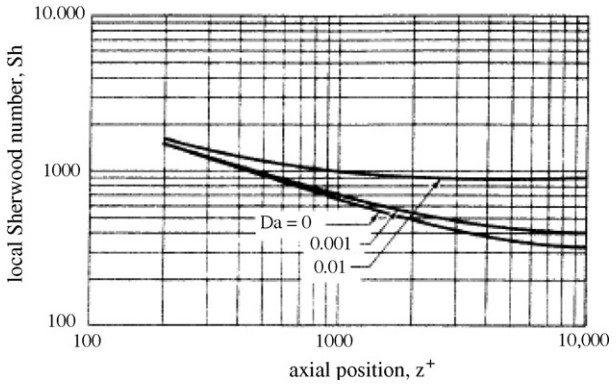

BSL2 Fig. 21.4-1. Local Sherwood number, *Sh*, given in BSL2 ([1], p. 662) for fully developed turbulent tube flow with $Re = 10000$, $Sc = 200$, and $Da = 0$, 0.001, and 0.01.

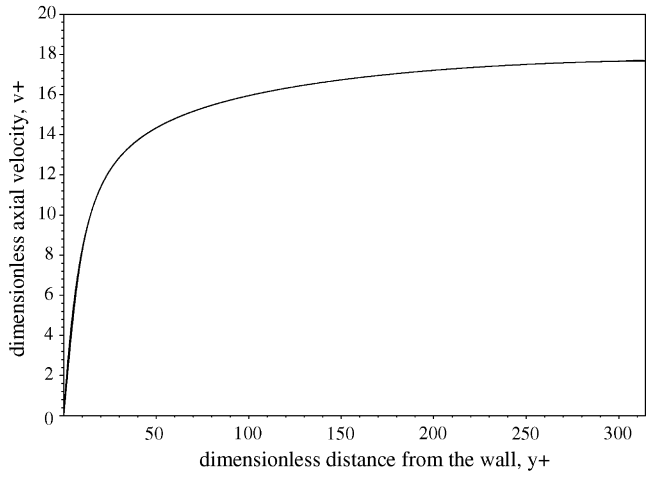

Fig. 1. Dimensionless time-smoothed axial velocity, $v^+(y^+)$, for fully developed turbulent tube flow with $Re = 10000$ and $f = 0.00791$. Values from the numerical solution of BSL2 Eqs. (21.4-13) and (21.4-14) and those from the 20-degree polynomial fit are indistinguishable. The maximum dimensionless distance is $y^+ = R^+ = 314.44$.

enhancements at large z^+ due to the presence of the homogeneous and irreversible chemical reaction (cases where $Da > 0$). Given Prof. Stewart's passing in 2006, the sketchy details of the solution procedure, and the limited results presented in BSL2, it is likely that the chemical engineering relevance and impact of this important mass transfer problem will not be fully appreciated.

In this communication the author provides: (1) a fully documented procedure for the numerical solution of BSL2 Eqs. (21.4-12)–(21.4-14) given the original values of $Re = 10000$, $Sc = 200$, and $Da = 0$, 0.001, and 0.01; (2) the dimensionless axial velocity profile v^+ for steadily driven turbulent flow in a smooth, 3 cm inner diameter tube (identical to that used in the BSL2 calculations); (3) the dimensionless molar concentration of solute A, C, at various radial and axial positions into the mass transfer zone; (4) *Sh* values at z^+ positions well outside the range of that shown in BSL2 Fig. 21.4-1 using a *single numerical simulation*, so that the limiting behavior of *Sh* for several *Da* may be better appreciated; and (5) a comparison of the mass transfer enhancement factors (ratio of the asymptotic *Sh* with chemical reaction to that without reaction) predicted by BSL2 Eqs. (21.4-12)–(21.4-14) and by other relevant studies in the literature. The results obtained in this study constitute a comprehensive supplement to those given in BSL2, and should be of interest to researchers in the fields of turbulent mass transfer, chemical reaction kinetics, and reactor design.

2. Mathematical formulation and solution strategy

Even though BSL2 Eq. (21.4-12) is formulated in terms of r^+ and z^+ as independent variables, this author solved for the dimensionless molar concentration C in terms of y^+ and x, with $y^+ = R^+ - r^+$ and x being a transformed dimensionless axial distance into the mass transfer zone, $x = \log_{10}(z^+ + 1)$. The dimensionless mass conservation equation for species A in terms of y^+ and x is given below, where use has been made of the chain rule to transform the left side concentration derivative in BSL2 Eq. (21.4-12) [for ease of computation, Eq. (1) was multiplied through by $(R^+ - y^+)$]:

$$v^+ \left(\frac{10^{-x}}{\ln 10}\right) \frac{\partial C}{\partial x} = \left(\frac{1}{R^+ - y^+}\right) \frac{\partial}{\partial y^+} \left[(R^+ - y^+) \left(\frac{1}{Sc} + (l^+)^2 \left| \frac{dv^+}{dy^+} \right| \right) \frac{\partial C}{\partial y^+} \right] - Da\, C \qquad (1)$$

The (y^+, x) coordinates allowed the numerical algorithm to start at the fluid side of the tube wall interface ($y^+ = 0$), which has a constant molar concentration of A, and to traverse a compressed axial length scale with $x(0) = 0$ and a reasonable number of increments to attain large values of z^+. As a first step, the dimensionless axial velocity profile, $v^+(y^+)$, was obtained from $y^+ = 0$ to $y^+ = R^+ = 314.44$ (see calculation under "Nomenclature") by numerically integrating BSL2 Eqs. (21.4-13) and (21.4-14) with $v^+(0) = 0$ (no-slip at the wall) and $dv^+/dy^+(R^+) = 0$ (symmetry at the tube centerline) using a standard Maple® solver for boundary-value problems with mesh adaptation, a maximum absolute error of 10^{-6}, and 30 digits preserved before truncation in all calculations (Waterloo, Ontario, Canada). Twenty one (y^+, v^+) data pairs, evenly-spaced across the radius of the tube, were obtained from the calculated axial velocity profile and least-square-fitted with a 20-degree polynomial, yielding a continuous and differentiable function $v^+(y^+)$ in $0 \le y^+ \le R^+$ [to be subsequently inserted in Eq. (1)]. Fig. 1 shows the numerical solution and the fitted values, which are indistinguishable. Note that the largest variation in the time-smoothed axial velocity occurs near the wall, the expected behavior for fully developed turbulent tube flow. The fitted velocity profile and its first y^+-derivative were then fed to a Maple® centered-based, finite-difference algorithm which solved Eq. (1) for $C(y^+, x)$ throughout a rectangular grid of 2000 increments in y^+ ($0 \le y^+ \le R^+$) and 200 increments in x ($0 \le x \le 8$). The number of both increments was increased progressively from arbitrary baseline values to the stated levels to ascertain the stability of

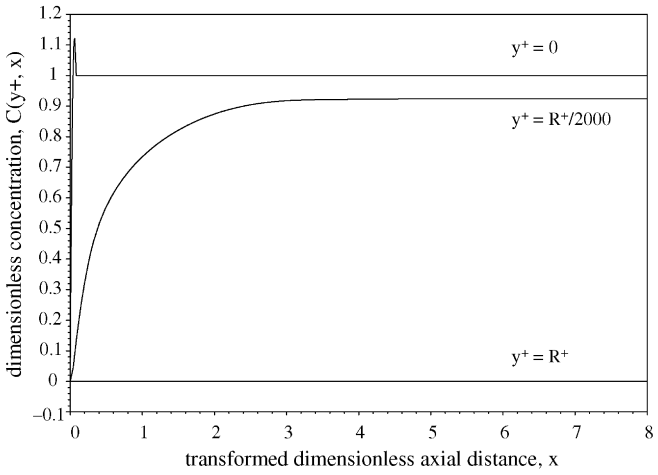

Fig. 2. Dimensionless molar concentration of solute A, $C(y^+, x)$, for $Da = 0$ (no reaction) at $y^+ = 0$ (fluid side of the wall interface), $y^+ = R^+/2000$ (first increment in y^+), and $y^+ = R^+$ (tube centerline) for fully developed turbulent flow. These profiles were obtained from the numerical solution of Eq. (1) and BSL2 Eqs. (21.4-13) and (21.4-14), along with the boundary conditions indicated in the text. The ordinate scale was chosen for clarity. $R^+ = 314.44$.

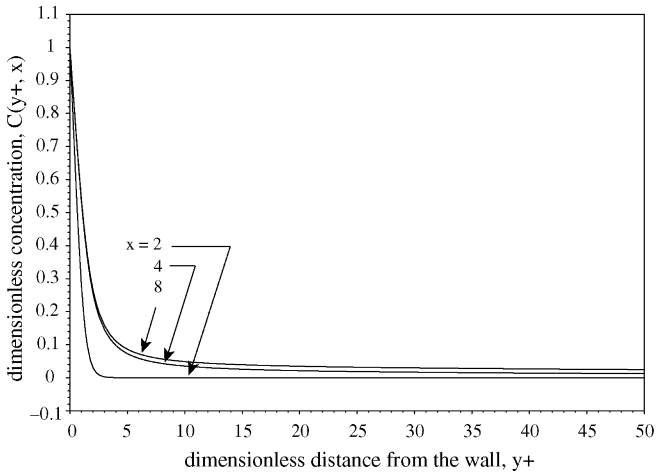

Fig. 3. Dimensionless molar concentration of solute A, $C(y^+, x)$, for $Da = 0$ (no reaction) at cross-sectional planes $x = 2$, 4, and 8 for fully developed turbulent tube flow. These profiles were obtained from the numerical solution of Eq. (1) and BSL2 Eqs. (21.4-13) and (21.4-14), along with the boundary conditions indicated in the text. Both scales were chosen for clarity.

the solution, with 30 digits preserved before truncation in all calculations. The boundary conditions in the (y^+, x) coordinates were $C(y^+, 0) = 0$ at the inlet of the mass transfer zone, $C(0, x) = 1$ on the fluid side of the wall interface (assumes instantaneous equilibration of the fluid with the solid A at the wall without partitioning), and $\partial C/\partial y^+(R^+, x) = 0$ (symmetry) at the tube centerline. The solution and associated plots depicting $C(y^+, x)$ for each value of Da took an average of 3 h to generate on a desktop personal computer (Gateway E Series, Intel® Pentium® 4 CPU, 2.67 GHz, 512 Mb RAM, Irvine, CA).

3. Comprehensive mass transfer results and discussion

Fig. 2 shows a typical $C(y^+, x)$ plot for the case $Da = 0$ (no reaction). The three curves are for the following representative dimensionless distances: $y^+ = 0$ (fluid side of the wall interface), $y^+ = R^+/2000$ (first increment in y^+), and $y^+ = R^+$ (tube centerline). The calculated curve for $y^+ = 0$ shows a concentration overshoot very close to the tube inlet ($z^+ = x = 0$), a common occurrence in the numerical solution of partial differential equations with discontinuous boundary conditions [3]. In this case, the boundary condition in z^+ represents a step increase in concentration across the plane $z^+ = 0$ at the tube wall, which affects the solution of Eq. (1) in the vicinity of (0, 0). The usual strategies for dealing with such overshoots are to concentrate grid points near the discontinuity (leading to variable increments) or to increase the total number of grid points keeping the increments uniform. The second approach was tried in the present study, resulting in a sharper overshoot very close to the tube inlet (data not shown). However, the maximum, unrealistic concentration of $C \sim 1.12$ was unaffected by such changes. The $y^+ = R^+/2000$ curve in Fig. 2 shows a steep increase in concentration near the tube inlet, followed by a flat profile for $x > 4$. Finally, the $y^+ = R^+$ curve shows similar behavior to the $y^+ = R^+/2000$ curve, but the non-zero concentration levels are extremely low [$C(R^+, 8) \sim 10^{-13}$] to be visible with the ordinate scale chosen. For the cases where $Da > 0$, all curves were found to be qualitatively similar to those in Fig. 2 (including the overshoot in the $y^+ = 0$ curve), but the concentration levels of the $y^+ = R^+/2000$ and $y^+ = R^+$ curves were lower due to the presence of the chemical reaction in the tube fluid. The three curves shown in this figure should give the reader good insight on the functionality of the local Sherwood number with z^+ and Da, as these concentrations enter directly in the Sh calculation to be discussed below.

Fig. 3 shows $C(y^+, x)$ for $Da = 0$ (no reaction) and $0 \le y^+ \le 50$ at three cross-sectional planes located at $x = 2$, 4, and 8. The largest changes in the fluid's solute concentration occur close to wall up to $x \sim 4$. For the cases where $Da > 0$, the curves fall off from $C = 1$ at $y^+ = 0$ in qualitatively similar fashion, but attain smaller values far from the wall than those in Fig. 3 due to the presence of the chemical reaction in the tube fluid.

Fig. 4 shows the local Sherwood number, Sh, as a function of the dimensionless axial distance into the mass transfer zone [plotted as Sh versus $\log_{10}(z^+)$ for convenience] for $Da = 0$, 0.001, and 0.01. The concentration derivative needed in the Sh calculation (equation given under "Nomenclature") was obtained from the concentration at the first increment in y^+ minus that at $y^+ = 0$ divided by the y^+-distance between the points ($R^+/2000$). This figure extends the z^+ scale in BSL2 Fig. 21.4-1 by four orders of magnitude to the right [$4 \le \log_{10}(z^+) \le 8$] and three to the left [$-1 \le \log_{10}(z^+) \le 2$] using a *single numerical simulation*. Although Sh remains unchanged for $\log_{10}(z^+) > 4$, the use of the full range [$-1 \le \log_{10}(z^+) \le 8$] demonstrates the stability of the solution, which may be advantageous when considering other physical situations or parameter settings. This positive feature of the solution is directly related to the use in this study of the transformed dimensionless axial distance x instead of z^+. Fig. 4 is qualitatively similar to BSL2 Fig. 21.4-1, but significant quantitative differences exist between the two, including the axial position where the curves merge and the asymptotic value of Sh for $Da = 0.01$ (~900 in BSL2 Fig. 21.4-1 versus

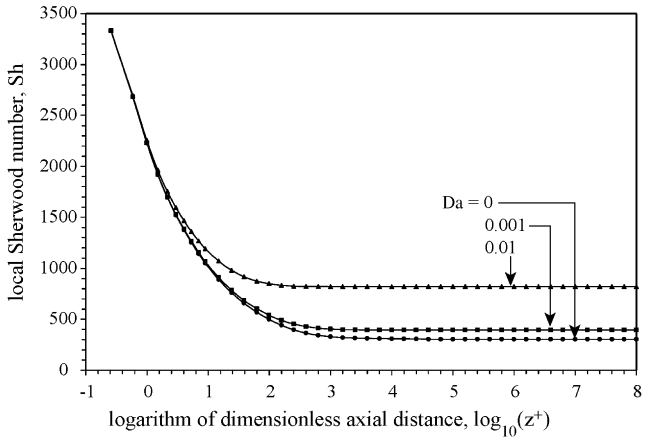

Fig. 4. Local Sherwood number, *Sh*, as a function of z^+ for $Da = 0$, 0.001, and 0.01. *Sh* is plotted versus $\log_{10}(z^+)$ to allow easy comparison of the results with BSL2 Fig. 21.4-1. The solid lines are smoothed representations of the *Sh* values calculated at specific z^+ locations (shown by symbols). This plot extends the range of z^+ in BSL2 Fig. 21.4-1 by four orders of magnitude to the right [$4 \le \log_{10}(z^+) \le 8$] and three to the left [$-1 \le \log_{10}(z^+) \le 2$] using a *single numerical simulation*. This shows the stability of the solution over the entire range [$-1 \le \log_{10}(z^+) \le 8$] and the usefulness of the x versus z^+ coordinate in the calculations.

822 in this study). Since details of the solution or additional data other than those presented in BSL2 ([1], p. 662) were never published, further quantitative comparison between the two figures is entirely speculative. Lending support to our calculations, Fig. 4 is also qualitatively similar to Fig. 11 for the local mass transfer coefficient in the Mitrovic and Papavassiliou study [4] to be discussed later.

Fig. 4 shows that, near the tube inlet, *Sh* is independent of *Da* since the rate of mass transfer of A from the wall into the fluid dominates the rate of reaction. Farther downstream, mass transfer from the wall slows down and the magnitude of *Da* has a marked effect on the asymptotic value of *Sh*, with significant enhancements observed in the $Da > 0$ cases (those involving chemical reaction) over the $Da = 0$ case (no reaction). One interesting finding was that the dimensionless axial distance needed for *Sh* to reach 95% of its asymptotic value (calculated at $x = 8$) decreased with increasing *Da* as follows: $z^+ \sim 5.0R^+$ for $Da = 0$, $z^+ \sim 1.8R^+$ for $Da = 0.001$, and $z^+ \sim 0.25R^+$ for $Da = 0.01$.

Since mass transfer enhancement factors ϕ, defined as the ratio of the asymptotic *Sh* with chemical reaction to that without reaction, can have a considerable impact on industrial reactor design (to give an obvious example), Table 1 compares ϕ from several studies addressing the same turbulent mass transfer problem for values of *Re*, *Sc*, and *Da* identical to those used in this work. The ϕ values from Hanna et al. [5] are higher than those of our study by as much as 17%, but this is not surprising since their model neglects the axial solute convection term altogether (left side of BSL2 Eq. (21.4-12)). With this omission, the authors fail to account for the increase in the fluid's solute concentration with z^+ (clearly shown in Figs. 2 and 3), leading to erroneous values of *Sh*. On the other hand, the ϕ values of Mitrovic and Papavassiliou [4] differ by ~1% from those of our study. This is an interesting agreement because their numerical solution to the problem is based on an entirely different approach to ours. In their case, spectral methods were used to calculate the fully developed turbulent velocity profile from the corresponding equation of motion (direct numerical simulation without experimental correlations), followed by the statistical tracking of a continuous line of mass markers released from a flat channel wall. Although the data for comparison of Mitrovic and Papavassiliou [4] and ours are limited, it is certainly encouraging that the results appear to be model-insensitive as far as the key reactor design parameter ϕ is concerned. Improved turbulent flow models and more accurate experimental data on velocity and concentration profiles (with and without chemical reaction) should provide better estimates of mass transfer enhancement factors in the future. As a final thought, the straightforward BSL2 modelling approach to this problem may also be used to examine the following scenarios of wide interest to chemical engineers in academia and industry: spatially variable boundary conditions, solute partitioning at $y^+ = 0$, complex reaction kinetics, different turbulent flow models, and geometries other than cylindrical.

Table 1
Mass transfer enhancement factors ϕ in turbulent tube flow predicted by several studies for $Re = 10000$, $Sc = 200$, and *Da* as indicated[a]

Da	Asymptotic *Sh* from this work[b]	ϕ		
		Eq. (10) [5]	Eq. (22b) [4]	This work
0	305.5[c]	–	–	–
0.001	395.5	1.382	1.285	1.295
0.01	821.6	3.179	2.657	2.690

[a] All numerical results are rounded to four significant figures.
[b] This is the local value calculated at the upper limit of the transformed dimensionless axial position, $x = 8$.
[c] For the curious reader, correlation *Q* of Perry et al. ([6], p. 5–63) gives an *average* $Sh = 281.0$ with $Re = 10000$ and $Sc = 200$ for fully developed turbulent tube flow. This correlation was obtained by Linton and Sherwood using experimental wetted-wall column and dissolution data (no reaction), and is valid for $2100 < Re < 35000$ and $0.6 < Sc < 3000$ [7]. Similarly, correlation *Y* ([6], p. 5–64) gives an *asymptotic* $Sh = 288.5$ for $Re = 10000$ and $Sc = 200$. This semiempirical correlation is based on a heat transfer analogy (fully developed turbulent tube flow with step increase in wall temperature and $Da = 0$) by Notter and Sleicher, and is valid for $2100 < Re < 100000$ and $Sc > 100$ [8]. Thus, there is reasonable agreement between the experimental *Sh* values of reference [6] and the theoretical value for $Da = 0$ from this study.

Acknowledgement

The author thanks the BSL2 triumvirate of authors, with whom he has had many pleasant scholarly interactions over the last few years in the fields of transport phenomena and the history of science.

References

[1] R.B. Bird, W.E. Stewart, E.N. Lightfoot, Transport Phenomena, second ed. (revised), John Wiley & Sons, Inc., New York City, NY, 2007, pp. 659–663.
[2] O.T. Hanna, O.C. Sandall, P.R. Mazet, Heat and mass transfer in turbulent flow under conditions of drag reduction, AIChE J. 27 (1981) 693–697.
[3] A. Jeffrey, Advanced Engineering Mathematics, Harcourt/Academic Press, Burlington, MA, 2002, pp. 540, 563, 564, 587, and 1012–1014.
[4] B.M. Mitrovic, D.V. Papavassiliou, Effects of a first-order chemical reaction on turbulent mass transfer, Int. J. Heat Mass Transfer 47 (2004) 43–61.

[5] O.T. Hanna, O.C. Sandall, C.L. Wilson, Mass transfer accompanied by first-order chemical reaction for turbulent duct flow, Ind. Eng. Chem. Res. 26 (1987) 2286–2290.
[6] R.H. Perry, D.W. Green, J.O. Maloney, Perry's Chemical Engineers' Handbook, seventh ed., The McGraw-Hill Companies, Inc., New York City, NY, 1997, pp. 5-63–5-64.
[7] W.H. Linton Jr., T.K. Sherwood, Mass transfer from solid shapes to water in streamline and turbulent flow, Chem. Eng. Progr. 46 (1950) 258–264.
[8] R.H. Notter, C.A. Sleicher, The eddy diffusivity in the turbulent boundary layer near a wall, Chem. Eng. Sci. 26 (1971) 161–171.